Effects of Depalmitoylation on Physicochemical Properties of Rhodopsin†

Kenneth W. Traxler and T. Gregory Dewey*

Department of Chemistry, University of Denver, Denver, Colorado 80208

Received July 6, 1993; Revised Manuscript Received November 10, 1993®

ABSTRACT: In an effort to determine the functionality of palmitoylation in rhodopsin, a number of physicochemical properties of depalmitoylated rhodopsin were monitored. Approximately 70% of the rhodopsin was depalmitoylated in rod outer segments by a mild hydroxylamine treatment that resulted in minimal bleaching of rhodopsin. Subsequent purification by affinity chromatography could be used to remove hydroxylamine-bleached rhodopsin. Parallel physical studies were performed on both purified, detergent-solubilized rhodopsin and rhodopsin in rod outer segments. No effect was seen on the rate of metarhodopsin II formation for depalmitoylated rhodopsin. A small effect was seen in the biphasic behavior of the rate of retinal regeneration. The circular dichroism spectrum of depalmitoylated, purified rhodopsin was virtually identical to that of the native protein. These results suggest that depalmitoylation does not greatly affect the conformational structure of rhodopsin. Circular dichroism at 222 nm was used to monitor the thermal denaturation of depalmitoylated and native rhodopsin. A small but significant decrease in the thermal stability was observed for purified rhodopsin but no decrease in stability was observed for rhodopsin in rod outer segments. In both cases, the van't Hoff parameters showed an increase in positive enthalpy for denaturation relative to the native state. This is largely counterbalanced by an increase in positive entropy relative to the native states. The circular dichroism of the "denatured" state showed a high α-helix content. Depalmitoylated rhodopsin had a lower helix content than native protein in this high-temperature state. The changes in the thermodynamics upon depalmitoylation were attributed to structural changes in the denatured state.

Lipid modification of eukaryotic proteins has received considerable recent attention (for a review see Towler et al., 1988). Palmitoylation of rhodopsin was first demonstrated by O'Brien (1987). It occurs when palmitic acid and the sulfhydryl from a cysteine form a thioester linkage. In the case of rhodopsin, mass spectroscopic studies have shown that this post-translational modification has a high specificity for palmitates over other fatty acids (Papac et al., 1992). Additionally, rhodopsin can be labeled in rod outer segments[1] (ROS) with [^{3}H]palmitoyl CoA or with palmitic acid, CoA, and ATP (O'Brien & Zatz, 1984). While these results are suggestive of an enzymatic palmitoylation process, it has been demonstrated that palmitoylation can also occur non-enzymatically (O'Brien et al., 1987). The specific palmitoylation sites on rhodopsin were identified by Ovchinnikov et al. (1988) and shown to be located at Cys-322 and Cys-323. Subsequently, palmitoylation was demonstrated in other G-protein coupled receptor families (cf. O'Dowd et al., 1989). In these systems the covalently linked palmitate is often located in the cytoplasmic tail region. For rhodopsin, the location on the cytoplasmic tail is juxtaposed between the G-protein binding site and the phosphorylation sites involved in desensitization. A possible role of rhodopsin palmitoylation is to anchor the carboxyl tail to the membrane. Such a structure would create an additional extramembraneous loop and potentially could have profound implications for the signal transduction process. However, demonstration of the functionality of this modification has been controversial.

Khorana and co-workers mutated the palmitoylated cysteines to serines and expressed them in COS-1 cells (Karnik et al., 1988). After purification and detergent solubilization, these rhodopsin mutants showed no difference in the light-initiated activation of transducin. In a more extensive study, the palmitoylation stoichiometry of the wild-type and of a variety of mutants was established (Karnik et al., 1993). It was shown that wild-type rhodopsin expressed in COS-1 cells behaved similarly to rhodopsin in ROS. Again, no effect on G-protein activation was observed upon removing the palmitates. Also, these mutants showed normal visible absorbance spectra and were able to be regenerated with 11-*cis*-retinal in a manner similar to that of the wild-type. A Cys-323$^-$ mutant showed reduced phosphorylation by rhodopsin kinase. In total the mutagenesis results do not suggest a major functional role for palmitoylation. These are in contrast to results on the β-2 adrenergic receptor, where mutation of the single palmitoylation site greatly reduced the agonist-dependent stimulation of adenylate cyclase (O'Dowd et al., 1989).

In a different approach, Pepperberg and co-workers (Morrison et al., 1991; Pepperberg & Okajima, 1992) studied the effect of hydroxylamine on rhodopsin in native settings. It was shown that treatment with 1 M hydroxylamine would remove >75% of the palmitates while preserving 85% of the rhodopsin. In ROS, rhodopsin stripped of palmitates showed a 44% inhibition in the regeneration of the retinal and a 61% increase in GTPase activity. It was argued (Morrison et al., 1991) that the discrepancy between these results and the mutagenesis results might be due to the use of detergent-solubilizing conditions in the prior work (Karnik et al., 1993). Removal of the membrane might compromise the functionality of the lipid modification. For experiments done on intact retinae, decreases in phosphorylation of light-exposed rhodop-

† Supported by the NSF REU Program. This research was supported, in part, by NSF Grant DMB-9002084.

* To whom correspondence should be addressed.

® Abstract published in *Advance ACS Abstracts,* February 1, 1994.

[1] Abbreviations: CD, circular dichroism; CoA, coenzyme A; conA, concanavalin A–agarose; DTNB, 5,5′-dithiobis(2-nitrobenzoic acid); DTT, dithiothreitol; MII, metarhodopsin II; Octyl glucoside, *n*-octyl β-D-glucopyranoside; PIPES, piperazine-*N*,*N*′-bis(ethanesulfonic acid); ROS, rod outer segments.

0006-2960/94/0433-1718$04.50/0

sin were observed after hydroxylamine treatment (Pepperberg & Okajima, 1992). This result is consistent with the mutagenesis work. It should be noted that 1 M hydroxylamine may have a number of other chemical effects, especially on a complex system. It is known that hydroxylamine will form the retinal oxime from *all-trans*-retinal upon bleaching rhodopsin (cf. Hofmann et al., 1983). Such effects can be avoided only if all the hydroxylamine is successfully removed.

In the present work, the effects of depalmitoylation on physical properties of rhodopsin are examined. A hydroxylamine treatment is used to remove endogenous palmitates from rhodopsin in ROS. A parallel study is made comparing depalmitoylated rhodopsin in ROS to purified, detergent-solubilized rhodopsin. After depalmitoylation the rhodopsin is purified in the presence of octyl glucoside using conA affinity chromatography. Under these conditions, hydroxylamine-bleached protein remains bound to the column and only unbleached protein is recovered (Litman, 1982). The circular dichroism of hydroxylamine-treated rhodopsin was measured along with its thermal denaturation behavior. For purified rhodopsin, a slight decrease in thermal stability is observed upon depalmitoylation. A thermodynamic analysis of the denaturation data is presented. In addition to these parameters, the rates of retinal regeneration and of formation of the MII photobleaching intermediate were also examined. Slight effects were seen in these parameters. These results suggest that depalmitoylation results in local structural changes that leave protein–retinal interactions unaffected.

MATERIALS AND METHODS

Preparative Techniques. Dark adapted, frozen bovine retinas were purchased from George A. Hormel Co. (Austin, MN) or from Excel Co. (St. Louis, MO). Rod outer segments were isolated by the sucrose density gradient procedure of Smith et al. (1975) and stored frozen in sucrose buffer at −80 °C. The sucrose buffer was later removed by washing the ROS with 50 mM Tris acetate, pH 7.0. All procedures were performed in darkness or under a dim red light. For experiments involving ROS, samples were sonicated for 30 s in a bath type sonicator (Laboratory Supplies Co.). Rhodopsin was purified using conA affinity columns as described previously (Litman, 1982). Column buffers contained 50 mM octyl glucoside and this prevents elution of bleached rhodopsin from the conA column with α-methyl mannoside. To depalmitoylate the rhodopsin, ROS were treated with 1 M hydroxylamine and incubated with gentle agitation at 37 °C for 1 h. The ROS were then washed four times with 100 mM sodium phosphate, pH 7.0. To determine the extent of removal of the palmitates, the sulfhydryl content of rhodopsin in ROS was determined using Ellman's reagent (Habeeb, 1972). Assays were performed on ROS instead of purified rhodopsin because of the reduced number of accessible sulfhydryls in this case. This colorimetric assay monitors the absorbance of DTNB at 412 nm using an extinction coefficient of 14 300 M^{-1} cm^{-1}. The concentration of rhodopsin was measured by solubilizing unbleached ROS with phosphate buffer containing 50 mM octyl glucoside and monitoring the retinal absorbance. An extinction coefficient of 40 000 M^{-1} cm^{-1} at 500 nm was used for rhodopsin (Shichi, 1970). All UV–vis spectra were measured on a Beckman DU50 spectrophotometer. Sulfhydryl analysis consistently showed a free sulfhydryl content of 1.9 groups per rhodopsin. Hydroxylamine-treated ROS consistently showed 3.4 sulfhydryls per rhodopsin. Thus, approximately 70% of the palmitates are being removed by hydroxylamine treatment.

Circular Dichroism Measurements and Thermal Denaturation. All CD measurements were performed on a JASCO J-500C spectropolarimeter. The buffer used for all CD experiments was 100 mM sodium phosphate, pH 7.0. Octyl glucoside (50 mM) was included in buffers for purified rhodopsin samples. Samples were placed in a 1 cm water-jacketed CD cell from NSG Precision Cell, Inc. Temperature was controlled with a Haake FK2 circulating water bath equipped with a Haake PG11 programmer. Temperature increases were programmed to be 28 deg/h. Temperature was monitored inside the CD cell with an Fe–constantan thermocouple and the voltage was recorded on a Linear strip chart recorder. For experiments involving ROS, the CD cell was moved to within 2 cm of the photomultiplier tube. This was done to minimize light-scattering artifacts.

Retinal Regeneration. Rates of regeneration of bleached rhodopsin with 11-*cis*-retinal were monitored using the procedure of Cusanovich (1982). Briefly, absorbance was monitored at 500 nm for a bleached sample balanced against a bleached reference. The buffer contained 100 mM sodium phosphate, 1 mM DTT, pH 7.0. Solubilized solutions contained 50 mM octyl glucoside. Samples were bleached by exposure to a bank of fluorescence lights for 15 min. Temperature was controlled using a Neslab circulating bath attached to the cell block. Temperature was monitored using an Fe–constantan thermocouple. The reference was stabilized by the addition of hydroxylamine at an equimolar concentration with rhodopsin. This forms the retinal oxime and prevents regeneration of the retinal. Aliquots of 11-*cis*-retinal dissolved in ethanol were delivered to both the sample and the reference and the time-dependence of absorbance changes at 500 nm was monitored. The solvent never exceeded 0.5% of the sample volume. Absorbance changes at 500 nm were recorded on the strip chart recorder and subsequently digitized by hand. This data and the flash spectroscopic data (next section) were both analyzed on a PC using a nonlinear least squares fitting routine based upon the Marquardt procedure. The 11-*cis*-retinal was a gift from Dr. Rosalie Crouch.

MII Formation Kinetics. Flash spectroscopic experiments were performed using an instrument constructed in our laboratory. A PhaseR DL-1400 dye laser was used to photolyse the rhodopsin. Coumarin 504 obtained from Exciton, Inc. (Dayton, OH) was used as a laser dye as its output best matches the 500-nm absorbance peak of rhodopsin. The pulse width of this laser is 50 ns. The absorbance response was monitored at 390 nm using a 150-W Xenon arc lamp, an ISA Model H-20 monochrometer, and an EMI 9635 photomultiplier with a PPI62/3A14 preamp. A Ditric 390-nm interference filter was placed in front of the photomultiplier tube. Signals were stored and dumped to a floppy disk using a Nicolet 310 storage oscilloscope (1-μs response time). Temperature was controlled using a 1-cm water-jacketed absorbance cell thermostated using a Neslab circulating water bath. Samples typically had an optical density of 0.3 at 500 nm. The buffer contained 10 mM PIPES, 60 mM KCl, 20 mM NaCl, 2 mM $MgCl_2$, pH 7.0. Relatively low laser intensities were used and approximately 10% of the rhodopsin was bleached per laser flash.

RESULTS

Thermal Denaturation Studies. After hydroxylamine treatment of ROS, the ROS were either washed extensively or rhodopsin was detergent-solubilized and purified. The CD spectrum of the purified, hydroxylamine-treated rhodopsin was compared with that of purified, untreated rhodopsin.

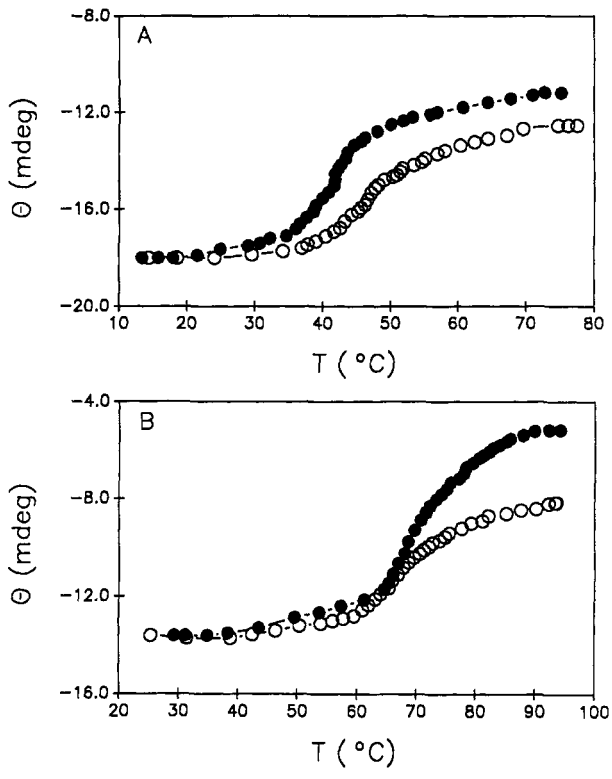

FIGURE 1: Thermal denaturation of purified rhodopsin (A) and rod outer segments (B) as monitored by changes in ellipticity at 222 nm. Ellipticity is plotted against temperature in degrees Celsius. Closed circles (●) are data for hydroxylamine-treated samples and open circles (○) are for untreated samples.

Comparable spectra were obtained and were similar to spectra reported earlier (Stubbs et al., 1976). These spectra were indicative of a protein with a high α-helix content. The molar ellipticity at 222 nm was determined for four different samples and average values of −18 800 ± 1700 and −18 200 ± 1400 deg cm^2/dmol were obtained for hydroxylamine-treated and untreated rhodopsin, respectively. Within error this is comparable to the previously determined value of −19 900 deg cm^2/dmol (Stubbs et al., 1976) and is in general agreement with other work (Ebrey & Yoshizawa, 1973; Shichi, 1973; Shichi et al., 1969). Typical thermal denaturation curves obtained when monitoring the ellipticity at 222 nm for hydroxylamine-treated and untreated purified rhodopsin are shown in Figure 1A. Shown in Figure 1B are the corresponding curves for ROS. It is clearly seen that purified, hydroxylamine-treated rhodopsin shows a decrease in thermal stability relative to untreated rhodopsin. Interestingly, a considerable α-helix content is still present even in the denatured state. Approximately 70% and 63% of the 222-nm signal remains at the high temperature limit for untreated and hydroxylamine-treated purified rhodopsin, respectively. Although this degree of α-helical content would be unusual for the denatured state of soluble proteins, the high temperature limit in this case will be referred to as the denatured state.

When measuring the CD melting curve, it was important to assess the reversibility of the process. When measured at a given temperature, the 222-nm intensity was constant with time, indicating that the kinetics of denaturation was not interfering with the measurements. This result suggests that an ongoing irreversible process was not occurring. However, if at the end of the melting experiment, the temperature was returned to a lower setting, the original CD intensity did not return. This indicates that either an irreversible denaturation or aggregation has taken place. If this process had occurred at the high temperature or during the cooling process, then the melting curve is unaffected and is accurate as observed. Protein denaturation models have been considered where the native and denatured state are in equilibrium and where the denatured state can slowly convert to a second, irreversible denatured state. These models, referred to as Lumry–Eyring models, can still be analyzed to give thermodynamics information (Sanchez-Ruiz, 1992), if the irreversible step is rate-limiting and only occurs above the transition temperature. Our constant time course at high temperatures suggests that, if irreversible denaturation is taking place, it follows a Lumry–Eyring mechanism. In such instances, an equilibrium thermodynamic model is permissible. Previous analysis of bacteriorhodopsin melting curves assumed such a model (Kahn et al., 1992).

The curves in Figure 1 were analyzed with a two-state model to give the van't Hoff enthalpy and entropy for denaturation. The fraction of protein that is not denatured, f, is given by

$$f = \frac{\theta - \theta_D}{\theta_N - \theta_D} \quad (1)$$

where θ is the ellipticity observed at a given temperature, θ_D is the ellipticity of the denatured state (high-temperature limit), and θ_N is the ellipticity of the native state (low-temperature limit). Often it is observed that θ_D is not well-defined and this is often attributed to a small temperature dependence of this parameter. This temperature dependence results in a sloping baseline and, in cases such as bacteriorhodopsin (Kahn et al., 1992), this results in a significant correction. This problem is not so severe in the present case. To avoid the subjectivity of drawing a sloping baseline, only the values at the extrema are used for the native and denatured states. Baseline corrections result in changes in the absolute values of the thermodynamic parameter, but do not change the trends that are observed. The equilibrium constant, K, for the native-denatured transition is then given by

$$K = \frac{1 - f}{f} \quad (2)$$

The van't Hoff enthalpy and entropy are determined from eq 3:

$$\ln K = \frac{-\Delta H^\circ}{RT} + \frac{\Delta S^\circ}{R} \quad (3)$$

The transition temperature (or "melting" temperature), T_m, is determined from the ratio of the enthalpy to the entropy, $\Delta H^\circ/\Delta S^\circ$. van't Hoff plots are shown in Figure 2 for representative melting curves of hydroxylamine-treated and untreated ROS and purified rhodopsin. These plots were fit with linear least-squares lines and in all cases showed correlation coefficients greater than 0.97. Data in Table 1 show average enthalpies, entropies, and transition temperatures determined from four melting curves. These results indicate that depalmitoylation of the protein increases both the positive enthalpy and entropy of denaturation. For purified rhodopsin, the favorable entropy increase is more than compensated by the unfavorable enthalpy, resulting in a T_m that is only 4 °C below that of native rhodopsin. ROS show a similar entropy–enthalpy compensation, but there is virtually no net change in T_m.

Retinal Regeneration. The time-course of retinal regeneration of bleached rhodopsin in sonicated ROS was monitored by the absorbance at 500 nm, A_{500}. It was previously postulated that a membrane environment was required to maintain the functional integrity of palmitoylation (Morrison et al., 1991).

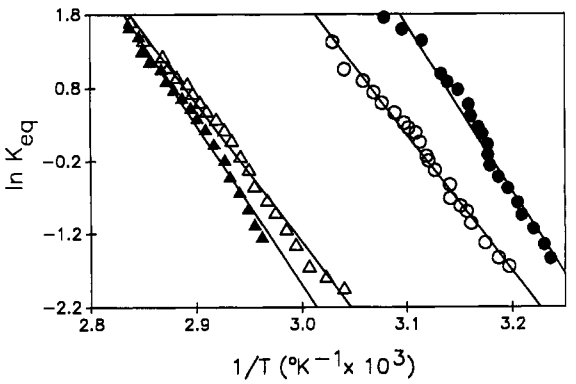

FIGURE 2: Arrhenius plot derived from the melting curves in Figure 1. The van't Hoff enthalpies and entropies in Table 1 are determined from the slopes and intercepts, respectively, of these plots. Lines are determined by linear regression. Circles (●, ○) are data for purified rhodopsin and triangles (▲, △) are data for ROS. Filled symbols are data for hydroxylamine-treated rhodopsin and open symbols are for untreated rhodopsin.

Table 1: Thermodynamic Parameters for Thermal Denaturation

	hydroxylamine-treated	untreated
	A. Purified Rhodopsin	
$\Delta H°$ (kcal/mol)	44.8 ± 1.7	37.4 ± 1.0
$\Delta S°$ (cal/K mol)	141 ± 0.3	116 ± 0.2
T_m (K)	318	322
	B. ROS	
$\Delta H°$ (kcal/mol)	44.1 ● 0.9	39.0 ± 0.8
$\Delta S°$ (cal/K mol)	129 ± 0.2	114 ± 0.2
T_m (K)	342	342

Consequently these experiments were performed in ROS. The observed signal was fit to the following double exponential function:

$$A_{500} = C_0 + C_1 e^{-t/\tau_1} + C_2 e^{-t/\tau_2} \quad (4)$$

where the fitted parameters are the amplitudes, C_i, and the lifetimes, τ_i. The temperature dependencies of the lifetimes fit the Eyring equation (eq 5):

$$\frac{1}{\tau} = (ekT/h)e^{-\Delta S^‡/R} e^{-E_a/RT} \quad (5)$$

where k and h are Boltzmann's and Planck's constants, respectively, and $\Delta S^‡$ and E_a are the activation entropy and enthalpy, respectively. Eyring plots of the two lifetimes for hydroxylamine-treated and untreated rhodopsin are shown in Figure 3. As can be seen, the effect of depalmitoylation is small. The activation entropies and energies determined from the intercepts and slopes of these plots are given in Table 2. It is seen that hydroxylamine treatment had virtually no effect on the fast component of regeneration. A slight effect is seen on the activation parameters for the slow component.

The Kinetics of MII Formation. The time course of formation of metarhodopsin II was observed by flash spectroscopy. Under the conditions of our experiments, the data could be fit with a single exponential. Other conditions provide evidence for the existence of two MII intermediates (cf. Straume et al., 1990) and concomitant biphasic kinetics. However, a wide range of conditions exist where only monophasic kinetics is observed (Williams & Baker, 1982). Figure 4 shows Eyring plots for the M-II formation for hydroxylamine-treated and untreated samples. Table 3 shows the activation parameters obtained from these plots. Both sonicated ROS and octyl glucoside-solubilized ROS were observed. The activation parameters were determined from

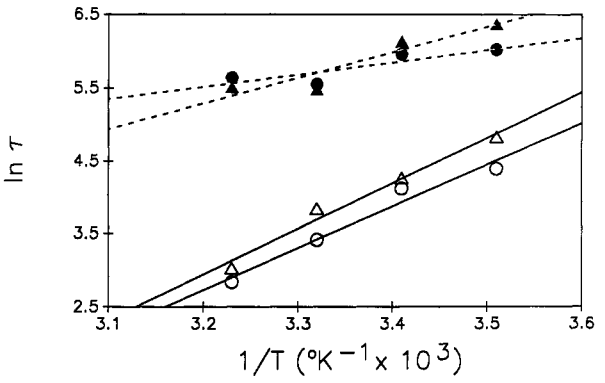

FIGURE 3: Eyring plots for the time constants associated with retinal regeneration. Two lifetimes were determined for this process. Solid lines represent the fast lifetime and dashed lines represent the slow lifetime. Data for hydroxylamine-treated ROS is shown by open (fast lifetime) and closed (slow lifetime) circles. Untreated ROS data is shown by open (fast lifetime) and closed (slow lifetime) triangles. Lines are determined by linear regression. Activation parameters derived from these plots are given in Table 2.

Table 2: Activation Parameters for Retinal Regeneration in ROS[a]

	hydroxylamine-treated	untreated
	Fast Lifetime	
E_a (kcal/mol)	11.5 ± 1.1	12.4 ± 0.9
$\Delta S^‡$ (cal/K mol)	31 ± 4	34 ± 3
	Slow Lifetime	
E_a (kcal/mol)	3.3 ± 0.9	6.9 ± 1.3
$\Delta S^‡$ (cal/K mol)	−0.4 ± 3	12 ± 5

[a] Standard deviation of parameters is determined from the linear regression.

Table 3: Activation Parameters for Metarhodopsin II Formation[a]

	hydroxylamine-treated	untreated
	Sonicated ROS	
E_a (kcal/mol)	30.3 ● 1.1	35.2 ± 1.5
$\Delta S^‡$ (cal/K mol)	153 ± 4	149 ± 7
	Solubilized ROS	
E_a (kcal/mol)	41.3 ± 1.2	39.6 ± 2.0
$\Delta S^‡$ (cal/K mol)	153 ± 4	149 ± 7

[a] Standard deviation of parameters is determined from the linear regression.

the slopes andintercepts of these plots. Within experimental error, the depalmitoylation of rhodopsin had no effect on this process.

DISCUSSION

In this work the effect of depalmitoylation on various physical properties of rhodopsin was determined. The properties observed were the circular dichroism spectra, thermal denaturation, retinal regeneration kinetics, and MII formation kinetics. The most significant effect of depalmitoylation was seen in the thermal denaturation. A small, but clearly observable (~4 °C), decrease in the transition temperature was observed in the purified system and little or no difference was observed in ROS. Analysis of the melting curves in both cases showed a significant enthalpy–entropy compensation effect. Thus, the palmitoylation loop has a minor effect upon protein stability. Since no difference was observed in the CD at room temperature upon depalmitoylation, the loss of protein stability must be a result of subtle, local structural effects. Apparently, these changes do not effect rhodopsin function in the processes under consideration. It is noteworthy that, for both rhodopsin and ROS, the CD in the denatured or

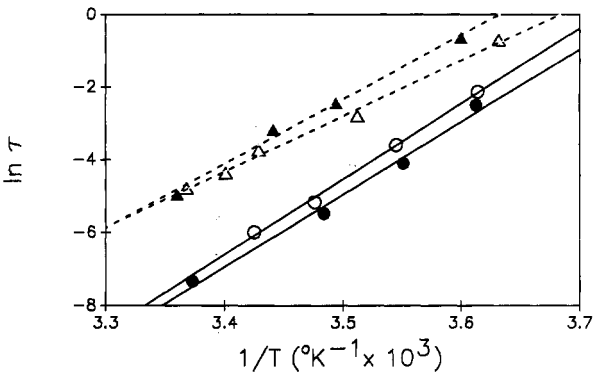

FIGURE 4: Eyring plots for the time constants associated with metarhodopsin II formation after flash excitation. A single lifetime was determined for this process. Open symbols represent hydroxylamine-treated samples. Closed symbols represent untreated samples. Triangles are data for sonicated ROS and circles are for solubilized ROS. Lines are determined by linear regression. Activation parameters derived from these plots are given in Table 3.

high-temperature state is considerably different for hydroxylamine-treated and untreated cases. For purified rhodopsin, after melting, 70% of the 222-nm signal remained for native rhodopsin while 63% remained for depalmitoylated rhodopsin. These CD results indicate that the effect of depalmitoylation is greater on the denatured state rather than on the native state.

It is of interest to compare the thermal denaturation results with those from the membrane protein bacteriorhodopsin (Kahn et al., 1992). For both rhodopsin and bacteriorhodopsin the final, high-temperature state (or "denatured" state) still shows considerable α-helical content. Thus, thermal denaturation in membrane proteins may represent quite a different process than for soluble proteins. Bacteriorhodopsin and rhodopsin both have seven membrane spanning regions. However, bacteriorhodopsin has extremely short loops connecting membrane spanning domains. They are not nearly as extensive as the loops in rhodopsin. Bacteriorhodopsin has a T_m of 90 °C while the T_m for purified rhodopsin is 49 °C and that for rhodopsin in ROS is 69 °C. In previous work (Kahn et al., 1992) the loops connecting membrane-spanning regions of bacteriorhodopsin were cleaved and the thermal stability of the resulting product was observed. Typically, loop cleavage destabilized the protein in a range from 5 to 20 °C. In our preliminary work (Moench et al., 1993) the membrane location of the palmitates modifying rhodopsin was established. Thus, palmitoylation anchors the carboxyl tail to the membrane, resulting in an additional loop in the structure. For purified rhodopsin, removing the anchor for this loop by depalmitoylation results in a 4 °C decrease in the transition temperature. Considering that approximately 70% of our sample is depalmitoylated by hydroxylamine treatment, the actual drop in T_m is comparable to that observed for loop cleavage in bacteriorhodopsin. However, it should be pointed out that for systems that exhibit strong entropy–enthalpy compensation, the transition temperature is not a particularly important parameter and the main manifestation of loop effects will be on the entropy.

The van't Hoff enthalpy and entropy for denaturation both show increases upon depalmitoylation. Often it is tempting to attribute thermodynamic changes to effects on the native state. However, to interpret these results, the stability of both the native and denatured states must be considered. In native rhodopsin it is conceivable that the modifying palmitates remain membrane bound and that the loop exists even in the denatured state. This would negate unfavorable entropy effects due to loop formation. The lack of an effect of depalmitoylation on a variety of physical properties, especially the molar ellipticity, suggests that the native conformation remains intact. Thus, the difference in thermodynamics should reflect the difference between palmitoylated and depalmitoylated protein in the denatured state. This can then be attributed to a difference in the energetics of forming the palmitoylation loop in the denatured state. With these assumptions, the thermodynamics of loop formation can be determined from Table 1, giving $\Delta H°_{loop,denatured} = -7.4$ kcal/mol and $\Delta S°_{loop,denatured} = -25$ eu for purified rhodopsin. The values obtained for ROS are $\Delta H°_{loop,denatured} = -5.1$ kcal/mol and $\Delta S°_{loop,denatured} = -15$ eu. From statistical mechanical treatments of loop formation in polymers, the entropy of loop closure can be calculated. This is given by

$$\Delta S_{loop} = -\nu R \ln N \qquad (6)$$

where N is the number of units in the loop and ν is a constant. For an excluded-volume polymer in which the loop occurs in the middle of a long polymer region (as opposed to on the end) the value of ν is generally accepted to be 2.4 in three-dimensions (cf. Chan & Dill, 1990). The number of residues from the top of the last membrane spanning regions to the palmitoylation site on rhodopsin is estimated to be 13. From eq 6 the contribution of loop formation to the entropy will be −12 eu. Thus, the loop effect would make a significant contribution to the observed entropy change. The presence of a comparable enthalpy effect suggests that other conformational factors should be considered. These factors doubtless will also have an entropic component and could be responsible for the remainder of the entropic contribution.

In summary, this work suggests that the main structural effect of palmitoylation is on the denatured conformation of rhodopsin. This is consistent with the lack of a significant alteration of a number of physical processes as a result of depalmitoylation. If the main effect of rhodopsin palmitoylation/depalmitoylation is on a denatured conformation, it is difficult to envision a biological role for palmitoylation. However, the thermally denatured conformation still maintains considerable α-helical structure, and it is conceivable that other physiologically relevant conformations may have structures similar to this state. It is also possible that the role for palmitoylation lies outside signal transduction and desensitization. This role may be related to packaging or turnover processes. Future studies will focus on elucidating the influence of palmitoylation on such biological processes.

ACKNOWLEDGMENT

We acknowledge the technical assistance of Dr. Robert D. Coombe on the flash spectroscopic experiments.

REFERENCES

Chan, H. S., & Dill, K. A. (1990) *J. Chem. Phys. 92*, 3118–3135.
Cusanovich, M. A. (1982) *Methods Enzymol. 81*, 443–447.
Ebrey, T., & Yoshizawa, T. (1973) *Exp. Eye Res. 17*, 545–556.
Habeeb, A. F. S. A. (1972) *Methods Enzymol. 25*, 457–464.
Hofmann, K. P., Emeis, D., & Schnetkamp, P. P. M. (1983) *Biochim. Biophys. Acta 725*, 60–70.
Kahn, T. W., Sturtevant, J. M., & Engleman, D. M. (1992) *Biochemistry 31*, 8829–8839.
Karnik, S. S., Ridge, K. D., Bhattacharya, S., & Khorana, H. G. (1993) *Proc. Natl. Acad. Sci. U.S.A. 90*, 40–44.
Litman, B. (1982) *Methods Enzymol. 81*, 150–153.
Moench, S. J., Stewart, D. M., & Dewey, T. G. (1993) *Biochemistry* (submitted).

Morrison, D. F., O'Brien, P. J., & Pepperberg, D. R. (1991) *J. Biol. Chem. 266*, 20118–20123.
O'Brien, P. J., & Zatz, M. (1984) *J. Biol. Chem. 259*, 5054–5057.
O'Brien, P. J., St. Jules, R. S., Reddy, T. S., Bazan, N. G., & Zatz, M. (1987) *J. Biol. Chem. 262*, 5210–5215.
O'Dowd, B. F., Hnatowich, M., Caron, M. G., Lefkowitz, R. J., & Bouvier, M. (1989) *J. Biol. Chem. 264*, 7564–7569.
Ovchinnikov, Y. A., Abdulaev, N. G., & Bogachuk, A. S. (1988) *FEBS Lett. 230*, 1–5.
Papac, D. I., Thornburg, K. R., Buellesbach, E. E., Crouch, R. K., & Knapp, D. R. (1992) *J. Biol. Chem. 267*, 16889–16894.
Pepperberg, D. R., & Okajima, T. I. (1992) *Exp. Eye Res. 54*, 369–376.
Sanchez-Ruiz, J. M. (1992) *Biophys. J. 61*, 921–935.
Shichi, H. (1970) *Biochemistry 9*, 1973–1977.
Shichi, H., Lewis, M. S., Irreverre, F., & Stone, A. (1969) *J. Biol. Chem. 244*, 529–536.
Smith, H. G., Stubbs, G. W., & Litman, B. J. (1975) *Exp. Eye Res. 20*, 211–217.
Straume, M., Mitchell, D. C., Miller, J. L., & Litman, B. J. (1990) *Biochemistry 29*, 9135–9142.
Stubbs, G. W., Smith, H. G., Jr., & Litman, B. (1976) *Biochim. Biophys. Acta 425*, 46–56.
Towler, D. A., Gordon, J. I., Adams, S. P., & Glaser, L. (1988) *Annu. Rev. Biochem. 57*, 69–99.
Williams, T. P., & Baker, B. N. (1982) *Methods Enzymol. 81*, 374–377.